

On the deceleration of relativistic jets in active galactic nuclei I: Radiation drag

V. S. Beskin^{1,2*} and A. V. Chernoglazov²

¹ *Lebedev Physical Institute, Russian Academy of Sciences, Leninsky prospekt 53, Moscow 119991, Russia*

² *Moscow Institute of Physics and Technology, Institutsky per. 9, Dolgoprudny 141700, Russia*

Accepted ... Received ...; in original form ...

ABSTRACT

Deceleration of relativistic jets from active galactic nuclei (AGNs) detected recently by MOJAVE team is discussed in connection with the interaction of the jet material with the external photon field. Appropriate energy density of the isotropic photon field which is necessary to decelerate jets is determined. It is shown that the disturbances of the electric potential and magnetic surfaces play important role in general dynamics of particle deceleration.

Key words: galaxies: active — galaxies: jets — quasars: general — radio continuum: galaxies — radiation mechanisms: non-thermal

1 INTRODUCTION

Recent progress in VLBI observations of relativistic jets outflowing from active galactic nuclei (Lobanov 1998; Cohen et al. 2007; Clausen-Brown et al. 2013; Kardashev et al. 2014) gives us new information concerning their physical characteristics and dynamics. In particular, rather effective deceleration of the jet material on the scale more than 50–100 pc was recently detected by MOJAVE team (Homan et al. 2015). We consider one possible explanation of such a deceleration connecting with the interaction of the jet with the external photon field. Both radiation drag and particle loading will be considered in detail on the ground of standard MHD approach, the first mechanism below and the second one in the accompany paper (Beskin & Nokhrina 2016).

Remember that it is the magneto-hydrodynamical (MHD) model that is now developed intensively in connection with the theory of relativistic jets outflowing from a rotating supermassive ($M \sim 10^8$ – $10^9 M_\odot$) black holes, which are thought as a ‘central engine’ in active galactic nuclei and quasars (Begelman, Blandford & Rees 1984; Thorne, Price & Macdonald 1986). In particular, it is the MHD model that is now the most popular in connection with the problem of the origin and stability of jets. Moreover, within last several years additional observational confirmations were found in favor of the MHD model such as the presence of the e^+e^- plasma (Reynolds et al 1996; Hirotani & Okamoto 1998) as well as the toroidal magnetic field (Gabuzda, Murrey & Cronin 2005). Finally, recent nu-

merical simulations (Komissarov et al. 2007; Porth et al. 2011; McKinney, Tchekhovskoy & Blanford 2012) demonstrate their very nice agreement with MHD analytical asymptotic solutions.

On the other hand, the density of photons in the vicinity of the central engine is high enough. This implies that the photon field may change drastically the characteristics of the ideal MHD outflow. For example, they may result in the particle loading, i.e., extensive e^+e^- pair creation (Svensson 1984), their acceleration by action of the radiation drag force for small enough particle energies as well as the deceleration of high energetic particles (Sikora et al 1996). In other words, in the self-consistent consideration the interaction of the magnetically dominated flow with the external photon field is to be taken into account.

Unfortunately, many years these two processes, i.e., MHD acceleration and the action of external photons, was developed separately. Only in the paper by Li, Begelman & Chiueh (1992) the first analytical step was done to combine them together. In particular, it was demonstrated how general equations can be integrated for conical geometry (which is impossible in general case). On the other hand, the consideration was produced in the given poloidal magnetic field. But under this assumption the fast magnetosonic surface (for cold flow) locates at infinity (Michel 1969; Kennel, Fujimura, Okamoto 1976; Lery et al 1998). As a result, it was impossible to analyze the radiation drag effect in the vicinity of the fast magnetosonic surface and the properties of the supersonic flow outside this surface.

Self-consistent disturbance of magnetic surfaces was included into consideration by Beskin, Zakamska & Sol (2004)

* E-mail: beskin@lpi.ru (VSB)

for high enough particle energy (when the radiation pressure is ineffective in particle acceleration). It was demonstrated that for magnetically dominated flow the drag force actually does not change the particle energy diminishing only the total energy flux. It was shown as well that the disturbance of magnetic surfaces becomes large only if the drag force changes significantly the total energy flux. Finally, recently Russo & Thompson (2013a,b) have considered the drag action on the magnetised outflow in gamma-busters where the radiation pressure can play the leading role in particle acceleration.

As to particle loading, several aspects of this process were considered by Svensson (1984); Lyutikov (2003); Derishev et al. (2003); Stern & Poutanen (2006). Even if the electron-positron pairs are created at rest (and, hence, they do not change the total energy and angular momentum flux), increasing of the particle flux inevitably decreases the mean particle energy. As a result, the particle loading can be considered as a rather effective mechanism of the deceleration of the jet bulk motion as well.

The main goal of this paper is to determine more carefully the photon drag action on the cylindrical magnetically dominated outflow. As a zero approximation (i.e., without radiation drag and particle loading) we use well-known analytical solution for cylindrical magnetically dominated MHD outflow (Istomin & Pariev 1994; Beskin 2009). As we are interested in the region far enough from the 'central engine', in what follows we consider the simple isotropic model of the radiation field (i.e. for energy density $U = U_{\text{iso}} = \text{const}$). Actually, our goal is just in evaluating U_{iso} which are necessary to explain the observable deceleration of jets on the scale 50–100 pc.

The paper is organized as follows. At first in Sect. 2 we discuss the very necessity to use two-fluid MHD approximation for highly magnetized winds and jets in the presence of the external photon field. In Sect. 3, starting from the basic two-fluid MHD equations we demonstrate how the drag force redistributing the electric charges results in the appearance of longitudinal electric field. It gives us the possibility to determine the change of particle energy. The beam damping resulting from particle loading is discussed in the accompany paper (Beskin & Nokhrina 2016). Finally, in Sect. 4 the main results of our consideration including astrophysical applications are formulated.

2 A PROBLEM

At first, let us formulate the main unsolved problem we are going to discuss. Up to now, both analytically (Michel 1969; Goldreich & Julian 1970; Heyvaerts & Norman 1989; Appl & Camenzind 1992; Beskin, Kuznetsova & Rafikov 1998; Beskin & Nokhrina 2006) and numerically (Komissarov 1994; Ustyugova et al 1995; Bogovalov & Tsinganos 1999; Komissarov et al. 2007; Tchekhovskoy et al. 2008, 2009; Bucciantini et al 2009; Porth et al. 2011; McKinney, Tchekhovskoy & Blanford 2012), the properties of highly magnetized winds and jets were mainly described within MHD approximation. Only recently the first steps were done using PIC numerical simulation (Sironi & Spitkovsky 2009; Beal, Guillori & Rose 2010), but these explorations are still in the very beginning.

It is convenient for us to introduce just now the main dimensionless parameters describing ideal MHD flow, namely, the particle multiplicity λ , the magnetization parameter σ_M , and the compactness parameter l_a . First, to describe the flow number density one can introduce so-called particle multiplicity λ

$$\lambda = \frac{n^{(\text{lab})}}{n_{\text{GJ}}}, \quad (1)$$

where $n_{\text{GJ}} = |\rho_{\text{GJ}}|/e$ and $\rho_{\text{GJ}} = \Omega_0 B_0 / (2\pi c)$ is the Goldreich & Julian (1969) charge density, i.e., the minimum charge density required for the screening of the longitudinal electric field in the flow. Here B_0 is the poloidal magnetic field in a jet and Ω_0 is the central engine angular velocity. As was shown by Nokhrina et al. (2015), for active galactic nuclei the multiplication parameter can be very large: $\lambda \sim 10^{11} - 10^{13}$.

Next, Michel (1969) magnetization parameter σ_M shows by how much the electromagnetic energy flux near the central engine can exceed the particle energy flux. The value σ_M corresponds to the maximal bulk Lorentz factor of the plasma that can be reached in the case where all the electromagnetic energy is transferred to the particle flow. In other words, σ_M is the maximum Lorentz factor that can be achieved in the magnetized wind. For cylindrical flow under consideration one can determine σ_M as

$$\sigma_M = \frac{\Omega_0 e B_0 r_{\text{jet}}^2}{4 \lambda m_e c^3}, \quad (2)$$

where r_{jet} is its transverse dimension of a jet.

The convenience of these two parameters stems from the fact that their product depends on the total energy losses W_{tot} only and, hence, can be determined from observations. Indeed, as was shown by Beskin (2010),

$$\lambda \sigma_M \sim \left(\frac{W_{\text{tot}}}{W_A} \right)^{1/2}, \quad (3)$$

where $W_A = m_e^2 c^5 / e^2 \approx 10^{17}$ erg/s. This value corresponds to minimum energy losses of a 'central engine' which can accelerate particles up to relativistic energies. Hence, we obtain $\lambda \sigma_M \sim 10^{14}$ for ordinary jets from AGN. Another representation of the product $\lambda \sigma_M$ is

$$\lambda \sigma_M \sim \frac{e E_r r_{\text{jet}}}{m_e c^2}, \quad (4)$$

where $E_r \sim (\Omega_0 r_{\text{jet}} / c) B_0$. As we see, this value corresponds to the total potential drop across the jet.

Finally, the compactness parameter

$$l_a = \frac{\sigma_T U_{\text{iso}} R}{m_e c^2} \quad (5)$$

is in fact the optical depth by Thomson cross section σ_T at a distance R in the photon field with energy density U_{iso} . Below, it will be important for us that the parameter l_a provide an upper limit of particle energy in the acceleration region. On the other hand, a large l_a is necessary for effective particle production.

It is necessary to stress that in this paper we consider only leptonic model of the relativistic jets. For this reason we normalize all the values on electron mass m_e . This approach is reasonable for very central parts of a jet connecting by magnetic field lines with the black hole horizon

(and, hence, loaded by secondary e^+e^- plasma generated by photon-photon conversion). It is in this region the numerical simulations mentioned above demonstrate regular magnetic field and energy flux. As to periphery part of a jet connecting with accreting disk, the special consideration including reconnection is necessary. This is beyond the scope of the present consideration.

Returning now to one-fluid MHD approach, it is necessary to stress that it has serious restriction. Indeed, well-known freezing-in condition $\mathbf{E} + \mathbf{v} \times \mathbf{B}/c = 0$ results in two consequences

$$E_{\parallel} = 0, \quad (6)$$

$$E_{\perp} < B, \quad (7)$$

namely, zero longitudinal electric field and smallness of the perpendicular electric field in comparison with magnetic one. Ferraro (1937) isorotation law, i.e., the conservation of so-called field angular velocity Ω_F (see below) along magnetic tubes is the mathematical formulation of this property. As a result, very large potential difference between the center and the boundary of a jet takes place up to the very end of a flow where the jet meets the external media (lobes in AGNs, HH objects in YSO, stellar wind in close TeV binaries).

On the other hand, it is clearly impossible to describe the interaction of external media with highly magnetized flow without including this potential drop into consideration. Indeed, neglecting E_{\perp} we do not include into consideration the role of the Poynting flux which is the main actor of our play. As a result, during such an interaction the domains with nonzero longitudinal electric field or with $E > B$ are to appear resulting in very effective particle acceleration (Beskin 2010). Nevertheless, up to now the role of the Poynting flux during the interaction with external media was considered only indirectly, say, by adding large enough toroidal magnetic field which energy density is similar to that of magnetized flow (Bogovalov et al. 2008, 2012; de la Cita et al. 2016). Remember that general properties of the MHD shock containing arbitrary Poynting flux were already formulated more than ten years ago (Double et al. 2004).

Effective particle acceleration can takes place even without external media. As was already demonstrated many years ago (Beskin, Gurevich & Istomin 1993; Beskin & Rafikov 2000), if there is some restriction on the longitudinal electric current circulating in the magnetosphere of radio pulsar, in the vicinity of the light cylinder $R_L = c/\Omega$ the region with $E > B$ appears. As a result, in the narrow region $\Delta r \sim R_L/\lambda$ the very effective particle acceleration is to take place up to the bulk Lorentz-factor $\Gamma \sim \sigma_M$. It is interesting that just such a sudden acceleration was recently supposed to explain pulse TeV radiation from Crab pulsar (Aharonian, Bogovalov & Khargulyan 2012)¹. Moreover, recent PIC modelling of the axisymmetric pulsar magnetosphere (Cerutti et al. 2015) also demonstrates very effective particle acceleration near the light cylinder up to $\gamma \sim \sigma_M$.

Here it is necessary to stress one very important

point. Not only one-fluid, but even two-fluid MHD approximation is not sufficient to describe the interaction of the highly magnetized flow with external media. As was shown by Beskin, Gurevich & Istomin (1993); Beskin & Rafikov (2000), effective particle acceleration in the domain with $E > B$ inevitably accompanied by vanishing of the radial velocity. This implies many-fluid regime which cannot be described analytically. The same concerns another dissipative processes, say, the magnetic reconnection which also discussed, mainly phenomenologically (Romanova & Lovelace 1992; Drenkhahn & Spruit 2002; McKinney & Uzdensky 2012; Golan & Levinson 2015; Bing & Huirong 2011; Levinson & Globus 2016) and numerically (Barkov & Kommisarov 2016; Del Zanna et al. 2016; Takamoto & Makoto 2013), in connection with the energy release in the highly magnetized flow.

In this paper we are not going to discuss the very interaction of a jet with external media, but try to evaluate the role of the external photon field in hydrodynamical retardation of a jet. In this case two-fluid approximation allows us to include into consideration self-consistently the longitudinal electric field and the disturbance of magnetic surfaces. As a result, one-fluid validity condition will be formulated.

3 RADIATION DRAG

3.1 Qualitative Consideration

At first, let us consider interaction of the magnetically dominated jet with the isotropic photon field qualitatively. Without the drag far enough from the rotation axis the particle motion along the jet corresponds to electric drift in radial electric E_r and toroidal magnetic $B_{\varphi} \gg B_z$ fields (Tchekhovskoy et al. 2008; Beskin 2009). It is clear that the drag force \mathbf{F}_{drag} directed along the jet results in the radial drift of electrons and positrons in opposite directions (see Fig. 1). The appropriate electric current can be evaluated as

$$j_r \sim \lambda \rho_{GJ} V_d, \quad (8)$$

where

$$V_d \sim c \frac{F_{\text{drag}}}{e B_{\varphi}} \quad (9)$$

is the drift velocity. Such a current is to diminish the toroidal magnetic field B_{φ} . Simultaneously, redistribution of charges is to diminish the radial electric field E_r . Both these processes result in reducing of the Poynting vector flux.

As in the magnetically dominated jet $E_r \approx B_{\varphi}$, one can write down the energy equation for the time-independent flow $\nabla \cdot \mathbf{S} = -\mathbf{j} \cdot \mathbf{E}$ as

$$\frac{c}{4\pi} \frac{dB_{\varphi}^2}{dz} \approx -j_r B_{\varphi}. \quad (10)$$

Using now relation (3) and evaluations $B_{\varphi}/B_z \sim r_{\text{jet}}/R_L$ and $W_{\text{tot}} \sim (c/4\pi) B_{\varphi}^2 r_{\text{jet}}^2$, we finally obtain for the characteristic retardation scale L_{dr}

$$L_{\text{dr}} \sim \sigma_M \frac{m_e c^2}{F_{\text{drag}}}. \quad (11)$$

The same evaluation can be directly obtained from the continuity equation $\nabla \cdot \mathbf{j} = 0$

¹ The title of this paper is 'Abrupt acceleration of a cold ultra-relativistic wind from the Crab pulsar'.

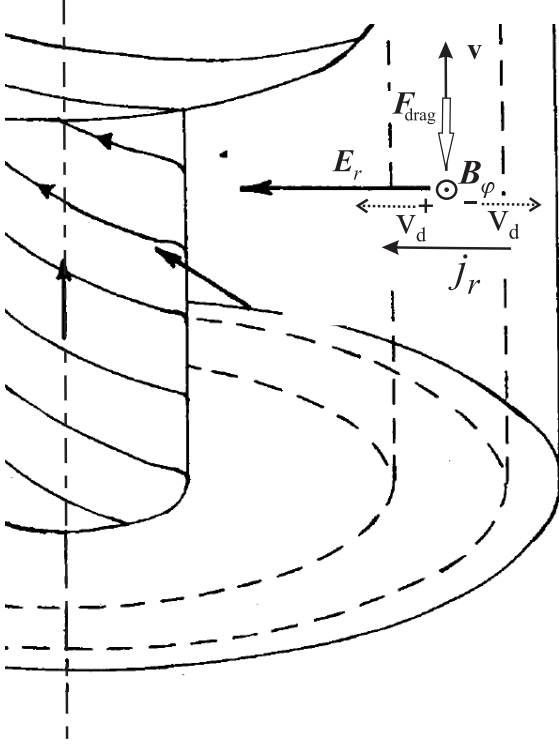


Figure 1. Drag force \mathbf{F}_{drag} results in the appearance of the radial drift current, redistribution of the electric charges, diminishing of the radial electric field and, finally, damping of the Poynting flux. The particle energy remains actually constant as the negative work of the drag itself actually equal to energy gain resulting from particle intersection of equi-potential surfaces.

$$\frac{j_r}{r_{\text{jet}}} \sim \frac{j_{\parallel}}{L_{\text{dr}}}, \quad (12)$$

where $j_{\parallel} \approx \rho_{\text{GJC}}$.

As we see, the work $A_{\text{dr}} = F_{\text{drag}} L_{\text{dr}}$ of the drag force F_{drag} on the scale L_{dr} (resulting in IC photons release of the jet energy flux)

$$A_{\text{dr}} \sim \sigma_{\text{M}} m_e c^2 \quad (13)$$

just equals to the particle energy corresponding to the total energy transfer from the electromagnetic Poynting flux to plasma outflow (Beskin & Rafikov 2000). This implies that our evaluation of the retardation scale is correct. But as this force acts actually perpendicular to the large toroidal magnetic field $B_{\phi} \sim (\Omega_0 r_{\text{jet}}/c) B_0$, in the first approximation the energy of particles remains constant. The point is that the energy loss $-F_{\text{drag}} v_z$ resulting from the drag force will be fully compensated by the energy $e E_r V_r$ gaining by particles due to their radial drift motion along radial electric field. Another words, the particle energy remains actually constant as the negative work of the drag itself actually equal to energy gain resulting from particle intersection of equi-potential surfaces.

Thus, as was firstly demonstrated by Beskin, Zakamska & Sol (2004), the drag force acting on plasma particles in the highly magnetized wind results in not the diminishing of particle energy but the diminishing of the Poynting flux as both the toroidal magnetic and radial electric field decrease along the jet.

As to particle deceleration, this process appears in the second order approximation when we have to include into consideration the diminishing of integrals of motion.

3.2 Cylindrical Flow

3.2.1 Basic Equations

In this section we consider the interaction of the cylindrical magnetically dominated jet with the isotropic photon field quantitatively. To have the possibility to analyze this process analytically, some simplifications will be used. At first, as was already stressed, we discuss leptonic model of relativistic jets. Second, below we consider pure cylindrical jet. This assumption is more serious than one can imagine at first glance. The point is that cylindrical geometry implies infinite curvature of the poloidal magnetic field. In this case there is well-known asymptotic behavior for particle Lorentz factors in the magnetically dominated flow $\Gamma \approx \Omega r_{\perp}/c$ which will be used in what follows.

Remember that for finite curvature radius R_c of the poloidal magnetic field another asymptotic solution $\Gamma \approx (R_c/r_{\perp})^{1/2}$ is possible. As was shown by Beskin, Zakamska & Sol (2004), see also Levinson & Globus (2016), under some conditions the photon drag increase the curvature radius R_c resulting in bulk acceleration of plasma particles. In addition, intrinsic instabilities of cylindrical jets (Benford 1981; Hardee & Norman 1988; Appl & Camenzind 1992; Lyubarskii 1999; Nalewajko & Begelman 2012; Tchekhovskoy & Bromberg 2016) also can change drastically the dynamics of interaction of photon field with magnetically dominated outflow. These processes are beyond the scope of our present consideration.

Finally, in what follows we consider magnetically dominated jet, i.e., the jet which does not reach their terminal Lorentz factor $\Gamma = \sigma_{\text{M}}$. It is not clear that the flow remains highly magnetized up to the distances 10-100 pc from the central engine under consideration. Nevertheless, this case is more interesting from physical point of view as it gives us the possibility to include into consideration the interaction of the photon field with Poynting flux. In Sect. 4 some astrophysical applications connecting with FRI–FRII classification will be given.

Thus, following Beskin, Zakamska & Sol (2004), we write down the set of time-independent Maxwell equations and two-fluid equations of motion for electron-positron plasma:

$$\nabla \cdot \mathbf{E} = 4\pi \rho_e, \quad \nabla \times \mathbf{E} = 0, \quad (14)$$

$$\nabla \cdot \mathbf{B} = 0, \quad \nabla \times \mathbf{B} = \frac{4\pi}{c} \mathbf{j}, \quad (15)$$

$$(\mathbf{v}^{\pm} \nabla) \mathbf{p}^{\pm} = e \left(\mathbf{E} + \frac{\mathbf{v}^{\pm}}{c} \times \mathbf{B} \right) + \mathbf{F}_{\text{drag}}^{\pm}. \quad (16)$$

Here \mathbf{E} and \mathbf{B} are the electric and magnetic fields, ρ_e and \mathbf{j} are the charge and current densities, and \mathbf{v}^{\pm} and \mathbf{p}^{\pm} are the speed and momentum of particles. Finally, \mathbf{F}_{drag} is the radiation drag force. For isotropic photon field (Blumenthal & Gould 1970; Rybicki & Lightman 1981)

$$\mathbf{F}_{\text{drag}}^{\pm} = -\frac{4}{3} \frac{\mathbf{v}}{v} \sigma_T U_{\text{iso}} (\gamma^{\pm})^2, \quad (17)$$

where γ^\pm are the Lorentz-factor of particles.

As is well-known, in the axisymmetric case one can express the electric and magnetic fields through three scalar functions, $\Psi(r_\perp, z)$, $\Omega_F(r_\perp, z)$, and $I(r_\perp, z)$

$$\mathbf{B} = \frac{\nabla\Psi \times \mathbf{e}_\varphi}{2\pi r_\perp} - \frac{2I(\Psi)}{cr_\perp} \mathbf{e}_\varphi, \quad (18)$$

$$\mathbf{E} = -\frac{\Omega_F(\Psi)}{2\pi c} \nabla\Psi. \quad (19)$$

Here $\Psi(r_\perp, z)$ is the magnetic flux, $I(\Psi)$ is the total electric current within the same magnetic tube, and $\Omega_F(\Psi)$ is the so-called field angular velocity (more exactly, the angular velocity of plasma drifting in electromagnetic fields).

For cylindrical outflow we have the following force-free solution of the general equations (14)–(16) (Istomin & Pariev 1994)

$$4\pi I(\Psi) = 2\Omega_F(\Psi)\Psi \quad (20)$$

corresponding to homogeneous poloidal magnetic field

$$B_z^{(0)} = B_0, \quad (21)$$

so that $\Psi^{(0)} = \pi B_0 r_\perp^2$, i.e., it does not depend on coordinate z ,

$$B_\varphi^{(0)} = -\frac{2I}{cr_\perp}, \quad (22)$$

$$E_r^{(0)} = B_\varphi^0, \quad (23)$$

and

$$B_r^{(0)} = 0, \quad B_z^{(0)} = B_0, \quad E_\varphi^{(0)} = 0, \quad E_z^{(0)} = 0. \quad (24)$$

It is important that this solution can be realised by massless particles moving along the jet with the velocity equal to that of light

$$v_z^{(0)} = c, \quad v_r^{(0)} = 0, \quad v_\varphi^{(0)} = 0. \quad (25)$$

Moreover, this solution is true for arbitrary profile of the angular velocity $\Omega_F(\Psi)$. In particular, one can consider the most interesting case $I(\Psi_{\text{jet}}) = \Omega_F(\Psi_{\text{jet}}) = 0$, when the total electric current flowing within the jet is equal to zero. For this reason, in what follows we consider $\Omega_F(r_\perp)$ as an arbitrary function.

As previously, in the cylindrical case we seek the first-order corrections for the case $v \neq c$ in the following manner:

$$n^+ = \frac{\Omega_0 B_0}{2\pi c e} [\lambda - K(r_\perp) + \eta^+(r_\perp, z)], \quad (26)$$

$$n^- = \frac{\Omega_0 B_0}{2\pi c e} [\lambda + K(r_\perp) + \eta^-(r_\perp, z)], \quad (27)$$

$$v_z^\pm = c [1 - \xi_z^\pm(r_\perp, z)], \quad (28)$$

$$v_r^\pm = c \xi_r^\pm(r_\perp, z), \quad (29)$$

$$v_\varphi^\pm = c \xi_\varphi^\pm(r_\perp, z). \quad (30)$$

Here $\Omega_0 = \Omega_F(0)$ and again $\lambda = n_e/n_{\text{GJ}}$ (1) is the multiplicity parameter. As was already stressed, for active galactic nuclei $\lambda \sim 10^{11} - 10^{13}$. Below, for simplicity, we consider λ as a constant. Besides,

$$K(r_\perp) = \frac{1}{4r_\perp} \frac{d}{dr_\perp} \left(r_\perp^2 \frac{\Omega_F}{\Omega_0} \right) \quad (31)$$

describes the charge density

$$\rho_e^0(r_\perp) = -\frac{\Omega_0 B_0}{\pi c} K(r_\perp) \quad (32)$$

and current density $j_z^0 = \rho_e^0 c$ transverse profiles. In particular, $K(0) = 1/2$ and

$$\pi \int_0^{r_{\text{jet}}} K(r') r' dr' = 0, \quad (33)$$

so both the total charge and total longitudinal current in the jet vanish. Finally, the disturbances of the electric potential $\Phi(r_\perp, z)$ and magnetic flux $\Psi(r_\perp, z)$ can be written as

$$\Phi(r_\perp, z) = \frac{B_0}{c} \left[\int_0^{r_\perp} \Omega_F(r') r' dr' + \Omega_0 r_\perp^2 \delta(r_\perp, z) \right], \quad (34)$$

$$\Psi(r_\perp, z) = \pi B_0 r_\perp^2 [1 + f(r_\perp, z)]. \quad (35)$$

It gives

$$B_r = -\frac{1}{2} r_\perp B_0 \frac{\partial f}{\partial z}, \quad (36)$$

$$B_\varphi = -\frac{\Omega_0 r_\perp}{c} B_0 \left[\frac{\Omega_F}{\Omega_0} + \zeta(r_\perp, z) \right], \quad (37)$$

$$B_z = B_0 \left[1 + \frac{1}{2r_\perp} \frac{\partial}{\partial r_\perp} (r_\perp^2 f) \right], \quad (38)$$

$$E_r = -\frac{\Omega_0 r_\perp}{c} B_0 \left[\frac{\Omega_F}{\Omega_0} + \frac{1}{r_\perp} \frac{\partial}{\partial r_\perp} (r_\perp^2 \delta) \right], \quad (39)$$

$$E_z = -\frac{\Omega_0 r_\perp^2}{c} B_0 \frac{\partial \delta}{\partial z}. \quad (40)$$

As we see, the values $|\delta| \sim 1$ and $|f| \sim 1$ just correspond to almost full dissipation of the Poynting flux.

Substituting now expressions (26)–(40) into (14)–(16), we obtain to the first order approximation the following linear system of equations:

$$- \frac{1}{r_\perp} \frac{\partial}{\partial r_\perp} (r_\perp^2 \zeta) = 2(\eta^+ - \eta^-) - 2[(\lambda - K)\xi_z^+ - (\lambda + K)\xi_z^-], \quad (41)$$

$$2(\eta^+ - \eta^-) + \frac{1}{r_\perp} \frac{\partial}{\partial r_\perp} \left[r_\perp \frac{\partial}{\partial r_\perp} (r_\perp^2 \delta) \right] + r_\perp^2 \frac{\partial^2 \delta}{\partial z^2} = 0, \quad (42)$$

$$r_\perp \frac{\partial \zeta}{\partial z} = 2[(\lambda - K)\xi_r^+ - (\lambda + K)\xi_r^-], \quad (43)$$

$$-r_\perp^2 \frac{\partial^2 f}{\partial z^2} - r_\perp \frac{\partial}{\partial r_\perp} \left[\frac{1}{r_\perp} \frac{\partial}{\partial r_\perp} (r_\perp^2 f) \right] = 4 \frac{\Omega_0 r_\perp}{c} [(\lambda - K)\xi_\varphi^+ - (\lambda + K)\xi_\varphi^-], \quad (44)$$

$$\frac{\partial}{\partial z} (\xi_r^+ \gamma^+) = -\xi_r^+ F_d(\gamma^+)^2 + 4 \frac{\lambda \sigma_M}{r_{\text{jet}}^2} \left[-\frac{\partial}{\partial r_\perp} (r_\perp^2 \delta) + r_\perp \zeta - r_\perp \frac{\Omega_F}{\Omega_0} \xi_z^+ + \frac{c}{\Omega_0} \xi_\varphi^+ \right], \quad (45)$$

$$\frac{\partial}{\partial z} (\xi_r^- \gamma^-) = -\xi_r^- F_d(\gamma^-)^2 - 4 \frac{\lambda \sigma_M}{r_{\text{jet}}^2} \left[-\frac{\partial}{\partial r_\perp} (r_\perp^2 \delta) + r_\perp \zeta - r_\perp \frac{\Omega_F}{\Omega_0} \xi_z^- + \frac{c}{\Omega_0} \xi_\varphi^- \right], \quad (46)$$

$$\frac{\partial}{\partial z} (\gamma^+) = -F_d(\gamma^+)^2 + 4 \frac{\lambda \sigma_M}{r_{\text{jet}}^2} \left(-r_\perp^2 \frac{\partial \delta}{\partial z} - r_\perp \frac{\Omega_F}{\Omega_0} \xi_r^+ \right), \quad (47)$$

$$\frac{\partial}{\partial z} (\gamma^-) = -F_d(\gamma^-)^2 - 4 \frac{\lambda \sigma_M}{r_{\text{jet}}^2} \left(-r_\perp^2 \frac{\partial \delta}{\partial z} - r_\perp \frac{\Omega_F}{\Omega_0} \xi_r^- \right), \quad (48)$$

$$\frac{\partial}{\partial z} (\xi_\varphi^+ \gamma^+) = -\xi_\varphi^+ F_d(\gamma^+)^2 + 4 \frac{\lambda \sigma_M}{r_{\text{jet}}^2} \left(-\frac{1}{2} \frac{cr_\perp}{\Omega_0} \frac{\partial f}{\partial z} - \frac{c}{\Omega_0} \xi_r^+ \right), \quad (49)$$

$$\frac{\partial}{\partial z} (\xi_\varphi^- \gamma^-) = -\xi_\varphi^- F_d(\gamma^-)^2$$

$$-4 \frac{\lambda \sigma_M}{r_{\text{jet}}^2} \left(-\frac{1}{2} \frac{cr_{\perp}}{\Omega_0} \frac{\partial f}{\partial z} - \frac{c}{\Omega_0} \xi_r^- \right). \quad (50)$$

Here again σ_M (2) is Michel magnetization parameter, and $F_d \approx l_a/R$ is the normalized radiation drag force

$$F_d = \frac{4}{3} \frac{\sigma_T U_{\text{iso}}}{m_e c^2}. \quad (51)$$

3.2.2 Zero MHD Approximation

As was already stressed, expression (20) can be considered as a zero force-free approximation describing cylindrical flow of massless particles. In the absence of a drag force we can now find exact MHD solution describing pure cylindrical flow as well. Indeed, as one can easily check, for

$$(\lambda - K) \xi_z^+ = (\lambda + K) \xi_z^-, \quad (52)$$

and

$$\xi_\varphi^\pm = x \xi_z^\pm \quad (53)$$

the cylindrical flow with $\xi_r^\pm = 0$, $\zeta = \delta = f = 0$ results in $\partial/\partial z = 0$. Here and below we use dimensionless distance from the axis $x_0 = \Omega_0 r_{\perp}/c$, and

$$x = \Omega_F(r_{\perp}) r_{\perp}/c. \quad (54)$$

As we see, in this case it is necessary to introduce a small difference in velocity of particles

$$\xi_z^+ - \xi_z^- = \frac{2K}{\lambda} \xi_z \sim \lambda^{-1} \xi_z, \quad (55)$$

where $\xi_z = (\xi_z^+ + \xi_z^-)/2$ is the hydrodynamical velocity. It is not surprising because equations (41)–(50) now describe the flow in MHD (not force-free) approximation. On the other hand, the mean particle energy is still the free function.

Below we use the following notations

$$\Gamma = \frac{\gamma^+ + \gamma^-}{2}, \quad G = \gamma^+ - \gamma^-, \quad (56)$$

$$P_+ = \frac{\xi_z^+ + \xi_z^-}{2}, \quad P_- = \xi_z^+ - \xi_z^-, \quad (57)$$

$$Q_+ = \frac{\xi_\varphi^+ + \xi_\varphi^-}{2}, \quad Q_- = \xi_\varphi^+ - \xi_\varphi^-, \quad (58)$$

Finally, as a free function we choose

$$\Gamma^2 = \Gamma_0^2 + x^2, \quad (59)$$

where $\Gamma_0 \sim 1$ is the free parameter. Expression (59) just corresponds the well-known analytical asymptotic solution obtained in many papers, see Beskin (2009) and references herein. Then, using relations (52)–(53), one can obtain

$$Q_{\pm} = x P_{\pm}, \quad (60)$$

$$P_- = 2 \frac{K}{\lambda} P_+, \quad (61)$$

$$Q_- = 2 \frac{K}{\lambda} Q_+, \quad (62)$$

$$G = -\Gamma^3 (1 - x^2 P_+) P_-, \quad (63)$$

where

$$P_+ = \frac{1}{\Gamma(\Gamma + \sqrt{\Gamma^2 - x^2})}. \quad (64)$$

In the last expression we put square root into the denominator to avoid the subtraction of two almost equal values Γ and $\sqrt{\Gamma^2 - x^2}$ in the numerator.

3.3 Drift Approximation

3.3.1 Two-fluid effects

Now we can use drag-free MHD solution (52)–(53) and (59)–(64) as a zero approximation, and evaluate the action of a drag force finding small disturbances in the linear approximation. It is clear that in this case all the disturbances including longitudinal electric field E_{\parallel} will be proportional to drag force F_d . Thus, under some conditions the electric force eE_{\parallel} acting on the charged particle could be larger than the retardation drag force F_d . In this case one of the species will be accelerated while another one will be decelerated more efficiently than by action of the drag force only resulting in full stop at some point. Thus, this condition corresponds to non-hydrodynamical regime. For this reason the determination of the ratio $eE_{\parallel}/F_{\text{drag}}$ is one of the main goal of our consideration.

Equations (41)–(50) can be simplified in the drift approximation. Indeed, well-known expression for drift velocity

$$\mathbf{V}_{\text{dr}} = c \frac{(e\mathbf{E} + \mathbf{F}_{\text{drag}}) \times \mathbf{B}}{eB^2} \quad (65)$$

fixes two velocity components perpendicular to the magnetic field \mathbf{B} .

It is necessary to remember that in the presence of the any force \mathbf{F} having the longitudinal component to the magnetic field the expression (65) is not valid. On the other hand, moving into the reference frame in which the force \mathbf{F} is parallel to the magnetic field, one can find that

$$\frac{|V_d|}{c} = \frac{1 + \epsilon_{\perp}^2 + \epsilon_{\parallel}^2 - \sqrt{(1 - \epsilon_{\perp}^2)^2 + \epsilon_{\parallel}^2(2 + 2\epsilon_{\perp}^2 + \epsilon_{\parallel}^2)}}{2\epsilon_{\perp}}, \quad (66)$$

where $\epsilon_{\perp, \parallel} = F_{\perp, \parallel}/eB$, the direction of the drift velocity remaining the same. As we see, the difference with the standard expression (65) $|V_{\text{dr}}|/c = \epsilon_{\perp}$ is proportional to ϵ_{\parallel}^2 . Hence, in the linear approximation under consideration this correction can be neglected.

As a result, determining all the velocity components and substituting them into equations of motion (47)–(48), as it is shown in Appendix A, one can obtain

$$\begin{aligned} \frac{\partial \gamma^{\pm}}{\partial z} &= -\frac{(1 - x^2 P_+)^2}{(1 + x^2)} F_d (\gamma^{\pm})^2 \\ &\mp \frac{4\lambda \sigma_M}{r_{\text{jet}}^2} \frac{(1 - x^2 P_+)}{(1 + x^2)} \left(-r_{\perp}^2 \frac{\partial \delta}{\partial z} + r_{\perp}^2 \frac{\Omega_F}{\Omega_0} \frac{1}{2} \frac{\partial f}{\partial z} \right). \end{aligned} \quad (67)$$

Expression (67) (which is one of the key result of our consideration) can be also obtained directly if we remember that general expression

$$\frac{d\mathcal{E}}{dt} = (\mathbf{F}_{\text{drag}} + e\mathbf{E})\mathbf{v} \quad (68)$$

in the drift approximation (65) looks like

$$\frac{d\mathcal{E}}{dt} = (F_{\parallel} + eE_{\parallel})v_{\parallel}. \quad (69)$$

In other words, only longitudinal component of the force (and only longitudinal component of the velocity) can change particle energy. Appearance of the factors $(1 + x^2)^{-1}$ and

$$(1 - x^2 P_+) \approx \frac{\Gamma_0}{\Gamma} \ll 1 \quad (70)$$

just result from this property.

As we see, together with the drag force (first term) always diminishing particle energy, Eqn. (67) contains the action of longitudinal electric field E_{\parallel} having two sources. In addition to disturbance of the electric potential δ , longitudinal electric field E_{\parallel} is to appear due to disturbance of magnetic surfaces f . The last term obviously vanishes if

$$\delta = \frac{1}{2} \frac{\Omega_F}{\Omega_0} f, \quad (71)$$

i.e., if magnetic surfaces are equi-potential. Thus, one can conclude that self-consistent analysis of the longitudinal electric field is to include into consideration not only the disturbance of electric potential δ , but the disturbance of the magnetic surfaces f as well.

As was already stressed, all linear disturbances are to be proportional to the drag force F_d . To determine these dependencies let us introduce the values

$$g_+ = \frac{\delta\gamma^+ + \delta\gamma^-}{2}, \quad g_- = \delta\gamma^+ - \delta\gamma^-, \quad (72)$$

$$p_+ = \frac{\delta\xi_z^+ + \delta\xi_z^-}{2}, \quad p_- = \delta\xi_z^+ - \delta\xi_z^-, \quad (73)$$

$$q_+ = \frac{\delta\xi_\varphi^+ + \delta\xi_\varphi^-}{2}, \quad q_- = \delta\xi_\varphi^+ - \delta\xi_\varphi^-. \quad (74)$$

Substituting them into (41)–(50) we obtain

$$q_- = xp_-, \quad (75)$$

$$q_+ = xp_+ + \frac{1}{R_L} \frac{\partial}{\partial r_{\perp}} (r_{\perp}^2 \delta) - x_0 \zeta, \quad (76)$$

$$g_+ = -\Gamma^3 p_+ + x\Gamma^3 P_+ q_+ + \frac{1}{4} x\Gamma^3 P_- q_-, \quad (77)$$

$$g_- = -\Gamma^3 (1 - x^2 P_+) p_- + x\Gamma^3 P_- q_+, \quad (78)$$

$$g_+ = -\frac{(1 - x^2 P_+)^2}{1 + x^2} \Gamma^2 (F_d z), \quad (79)$$

$$g_- = -\frac{8\lambda\sigma_M(1 - x^2 P_+)}{1 + x^2} \frac{r_{\perp}^2}{r_{\text{jet}}^2} \left(\delta - \frac{1}{2} \frac{\Omega_F}{\Omega_0} f \right), \quad (80)$$

$$\zeta = -\frac{A}{\sigma_M} \Gamma^2 (F_d z) + 4K \frac{xx_0}{1 + x^2} \delta + 2K \frac{1 - x^2 P_+}{1 + x^2} f, \quad (81)$$

$$\frac{1}{r_{\perp}} \frac{\partial}{\partial r_{\perp}} \left[r_{\perp} \frac{\partial}{\partial r_{\perp}} (r_{\perp}^2 \delta) \right] + r_{\perp}^2 \frac{\partial^2}{\partial z^2} \delta - \frac{1}{r_{\perp}} \frac{\partial}{\partial r_{\perp}} (r_{\perp}^2 \zeta) = -2\lambda p_- + 4K p_+, \quad (82)$$

$$-r_{\perp}^2 \frac{\partial^2}{\partial z^2} (f) - r_{\perp} \frac{\partial}{\partial r_{\perp}} \left[\frac{1}{r_{\perp}} \frac{\partial}{\partial r_{\perp}} (r_{\perp}^2 f) \right] = 4\lambda x x_0 p_- - 8x_0 K q_+, \quad (83)$$

As is shown in Appendix A, the system of equations (75)–(83) can be rewritten as two second-order ordinary differential equations (A19)–(A20) for $D = x_0^2 \delta$ and $F = x x_0 f$ resulting in outside the light cylinder

$$\frac{d^2}{dx_0^2} \left(D - \frac{F}{2} \right) - \frac{16\lambda^2 \sigma_M}{\Gamma^3 x_{\text{jet}}^2} \left(D - \frac{F}{2} \right) + \dots = 0. \quad (84)$$

Hence, the physical branch of equations (A19)–(A20) corresponds to fast diminishing solution $(D - F/2) \rightarrow 0$ with the spacial scale $\Delta r_{\perp} \ll r_{\text{jet}}$, where

$$\Delta r_{\perp} = \frac{\Gamma^{3/2}}{4\lambda\sigma_M^{1/2}} r_{\text{jet}}. \quad (85)$$

Thus, for $\Delta r_{\perp} \ll r_{\text{jet}}$ (and for $\lambda\sigma_M \gg 1$) one can neglect l.h.s. of Eqn. (80). As we see, in this case we return

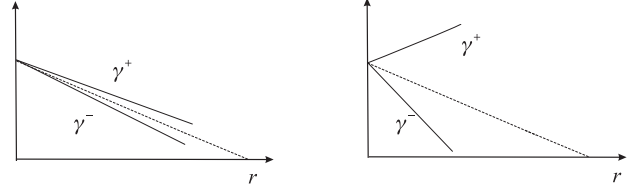


Figure 2. Hydrodynamical ($|g_-| \ll |g_+|$) and non-hydrodynamical ($|g_-| > |g_+|$) regimes of drag action. In the first case Lorentz-factors of electrons γ^- and positrons γ^+ actually coincide with the mean value Γ . In the last case one of the species accelerates while another one decelerates more efficiently than by action of the drag force only resulting in full stop at some point.

to one-fluid MHD condition (71). Finding now q_+ from (77) and ζ from (76), we obtain two equations for p_- and δ

$$2\lambda p_- - \frac{4K x x_0 P_+}{(1 - x^2 P_+)} \frac{1}{r_{\perp}} \frac{\partial}{\partial r_{\perp}} (r_{\perp}^2 \delta) + \frac{16K^2 (x^2 + 1 - x^2 P_+) x_0^2 P_+}{(1 + x^2)(1 - x^2 P_+)} \delta = \frac{4K x x_0 P_+}{(1 - x^2 P_+)} \frac{A\Gamma^2}{\sigma_M} (F_d z) - 2 \frac{A\Gamma^2}{\sigma} (F_d z), \quad (86)$$

$$4\lambda x x_0 p_- - \frac{8K x_0^2}{(1 - x^2 P_+)} \frac{1}{r_{\perp}} \frac{\partial}{\partial r_{\perp}} (r_{\perp}^2 \delta) + \frac{32K^2 x_0^3 x}{(1 - x^2 P_+)(1 + x^2)} \delta = \frac{8K x_0 x}{(1 - x^2 P_+)} \frac{A\Gamma^2}{\sigma} (F_d z). \quad (87)$$

Here

$$A(r_{\perp}) = \frac{r_{\text{jet}}^2}{r_{\perp}^2} \left[1 - \frac{(1 - x^2 P_+)^2}{1 + x^2} \right] \frac{\Omega_0}{\Omega_F}, \quad (88)$$

so that $x^2 A \sim x_{\text{jet}}^2 \gg 1$ ($A \sim 1$ for $x \sim x_{\text{jet}}$), and we neglect all the terms containing $\partial^2/\partial z^2$ (for small F_d the derivatives along the jet are small), x^{-2} and $(1 - x^2 P_+) \ll 1$. The full version is given in Appendix A.

3.3.2 Qualitative consideration

At first, let us discuss the result obtained above qualitatively; the appropriate numerical evaluations will be given in the next section. First, evaluating $r_{\perp}^{-1} \partial(r_{\perp}^2 \delta)/\partial r_{\perp}$ as δ , one can obtain

$$\delta = k_{\delta} \frac{A}{\sigma_M} \Gamma^2 (F_d z), \quad (89)$$

$$p_- = \frac{k_p}{\lambda\sigma_M} \frac{KA}{(1 - x^2 P_+)} \Gamma^2 (F_d z), \quad (90)$$

where $k_{\delta} \sim k_p \sim 1$. As we see, expression (89) for δ together with clear condition $|\delta| \sim 1$ for the full damping of the Poynting flux reproduces immediately our evaluation (11) for the length $L_{\text{dr}} = \sigma_M m_e c^2 / F_{\text{drag}}$; now it can be rewritten as

$$L_{\text{dr}} \sim \frac{\sigma_M}{\Gamma^2 F_d}. \quad (91)$$

Further, using expression (90) for p_- together with (75) and (77) one can obtain

$$g_- \sim \frac{A}{\lambda\sigma_M} \Gamma^5 (F_d z). \quad (92)$$

Together with (79) it gives

$$\frac{g_-}{g_+} \sim \frac{1}{\lambda \sigma_M} \frac{(1+x^2)A}{(1-x^2P_+)^2} \Gamma^3. \quad (93)$$

Relation (93) is actually our main result separating hydrodynamical and non-hydrodynamical regime of the drag force action. Indeed, for large enough multiplicity $\lambda > \lambda_*$, where

$$\lambda_* = \frac{x_{\text{jet}}^2 \Gamma^3}{\sigma_M (1-x^2P_+)^2}. \quad (94)$$

the difference in Lorentz-factors of electrons and positrons is negligible, and we deal with one-fluid MHD flow. On the other hand, for $|g_-| > |g_+|$ the drag force F_{drag} is smaller than the electrostatic one eE_{\parallel} . As a result, as is shown on Fig. 2, one of the species accelerates while another one decelerates more efficiently than by the action of the drag force only resulting in full stop at some point. It is clear that in the last case the very hydrodynamical description it now impossible. As the condition (94) can be rewritten as

$$\lambda \sigma_M = \frac{x_{\text{jet}}^2 \Gamma^5}{\Gamma_0^2}, \quad (95)$$

we see that according to (3) non-hydrodynamical regime can be realised for small $W_{\text{tot}} < W_*$, where

$$W_* = \frac{x_{\text{jet}}^4 \Gamma^{10}}{\Gamma_0^4} W_A, \quad (96)$$

where again $W_A = m_e^2 c^5 / e^2 \approx 10^{17}$ erg/s. The corresponding Poyting flux is less than

$$S_* = \frac{x_{\text{jet}}^2 \Gamma^{10}}{\Gamma_0^4} W_A, \quad (97)$$

Accordingly, in the non-hydrodynamical regime the distance L_{st} to the stop point can be evaluated as

$$L_{\text{st}} \sim \frac{\lambda \sigma_M}{\Gamma^4 F_d}. \quad (98)$$

Finally, in one-fluid approximation corresponding to condition $|g_-| \ll |g_+|$ we can write down

$$\frac{\partial}{\partial z} \Gamma = -\frac{(1-x^2P_+)^2}{1+x^2} F_d \Gamma^2. \quad (99)$$

Certainly, it is possible to use this solution for small disturbance of the Lorentz-factor Γ only. Nevertheless, we again can evaluate the distance L_{Γ} of the essential diminishing of the bulk particle energy $m_e c^2 \Gamma$ of the motion on the scale L

$$L_{\Gamma} \sim \frac{x_{\text{jet}}^2 \Gamma}{\Gamma_0^2 F_d}. \quad (100)$$

As we see, this distance is much larger than L_{dr} . It is not surprising as in the linear approximation, as was already stressed, the particle energies remain actually constant. For this reason it is impossible to use the value L_{Γ} as the evaluation of the retardation length.

3.3.3 Quantitative consideration

Finally, below we present the result of numerical integration of the linear system (86)–(87). Neglecting p_- and the derivatives $\partial/\partial z$, one can obtain the second-order ordinary differential equation for determination δ only. It looks like (see Appendix A for more detail)

$$2x \frac{d}{dx_0} \left[x_0 \frac{d}{dx_0} D \right] - 2x_0 \frac{d}{dx_0} \left[\frac{1}{x_0} \frac{d}{dx_0} \left(\frac{\Omega_0}{\Omega_F} D \right) \right] +$$

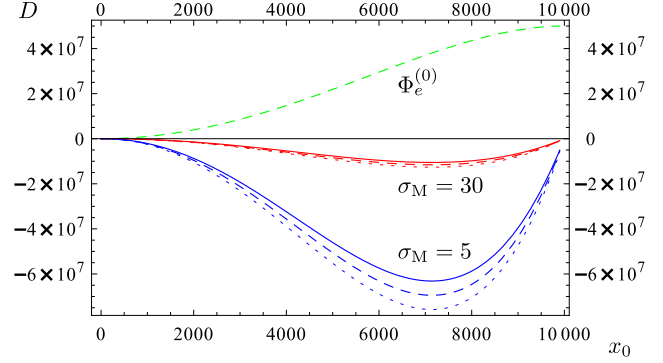


Figure 3. Solution $D = x_0^2 \delta$ of Eqn. (101) for $x_{\text{jet}} = 10^4$ and for different values σ_M . Solid, dashed and dotted lines of the same color correspond to three different value of F_{dz} : 1, 1.1, 1.2 respectively. Upper curve corresponds to undisturbed electric potential $\Phi_e^{(0)}$.

$$\begin{aligned} 8x \frac{d}{dx_0} \left[K \frac{(x_0 x + \Omega_0/\Omega_F - x^2 P_+ \Omega_0/\Omega_F)}{(1+x^2)} D \right] + \\ 8Kx_0 \frac{d}{dx_0} D - \frac{32K^2 x_0 (x^2 + 1 - x^2 P_+)}{x(1+x^2)} D \\ = -2x \frac{d}{dx_0} [x_0^2 \mathcal{G}] - 8Kx_0^2 \mathcal{G}, \end{aligned} \quad (101)$$

where $D = x_0^2 \delta$, $\mathcal{G} = A \Gamma^2 (F_d z) / \sigma_M$ and again $x_0 = \Omega_0 r_{\perp} / c$ and $x = \Omega(r_{\perp}) r_{\perp} / c$. As to angular velocity profile $\Omega_F(r_{\perp})$ which determines the coefficient K (31), we use the simplest relation

$$\Omega_F(r_{\perp}) = \Omega_0 \left(1 - \frac{r_{\perp}^2}{r_{\text{jet}}^2} \right) \quad (102)$$

corresponding to zero total electric charge and electric current within the jet $\Omega_F(r_{\text{jet}}) = 0$.

Additional remarks are to be done to boundary conditions. As is shown in Appendix B, to avoid longitudinal electric field on the jet axis it is necessary to put $D(0) = 0$. Together with the regularity condition at the light cylinder $x = 1$ it helps us to obtain the full solution of a problem.

As it is shown in Fig.3, solution of equation (101) gives negative values for the disturbance of the electric potential δ . This just implies that the disturbance δ resulting from drag force compensates gradually the electric potential of the jet (upper curve). Moreover, as is shown on Fig. 4, our evaluation (89) reproduces good enough the exact solution of Eqn. (101).

Finally, as, according to (71), disturbance of magnetic surfaces f is to be negative as well, one can rewrite the magnetic flux $\Psi(r_{\perp}, z)$ (35) as

$$\Psi(r_{\perp}, z) = \pi B_0 r_{\perp}^2 (1 - Cz), \quad (103)$$

where $C > 0$. It leads to appearance of a positive radial component of the magnetic field B_r (36), i.e., to decollimation of the jet². But as one can easily check, the width of the jet increases essentially only for $\delta \sim 1$ when almost all electromagnetic energy will be transferred into IC photons.

² We consider here the case $B_z > 0$.

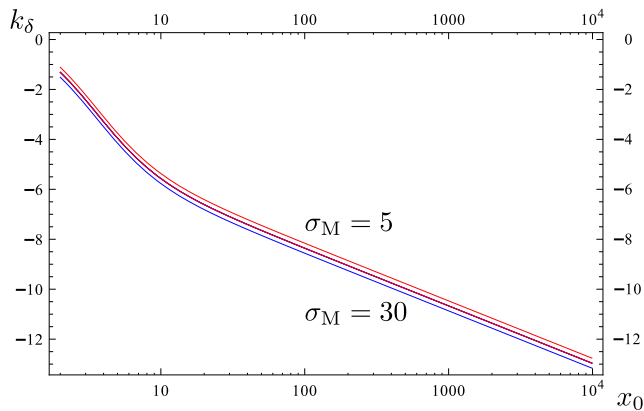


Figure 4. Dimensionless function k_δ which actually does not depend on magnetization parameter σ_M .

4 ASTROPHYSICAL APPLICATIONS AND DISCUSSIONS

Thus, we have demonstrated how for simple geometry it is possible to determine the small correction of the one-fluid ideal outflow resulting from radiation drag force. In comparison with the paper by Li et al (1992), both the disturbance of magnetic surfaces and electric potential were included into consideration self-consistently. As a result, the possibility arises to find the tendency of the drag action on the ideal MHD magnetically dominated outflow as well as to evaluate the conditions when this disturbance becomes large.

Let us try now to evaluate the real role of radiation drag in dynamics of relativistic jets in active galactic nuclei. As the energy density U_{iso} at the distance R from the ‘central engine’ with the total luminosity L_{tot} can be estimated as $U_{\text{tot}} \sim 10^{-3} \text{ erg/cm}^3$ at the distance $R = 10 \text{ pc}$. Assuming that $U_{\text{iso}} \sim 0.1 U_{\text{tot}} \sim 10^{-4} \text{ erg/cm}^3$, see, e.g., Joshi et al (2014)), one can evaluate the length of hydrodynamical retardation L_{dr} given by (11) as

$$L_{\text{dr}} \sim 300 \left(\frac{\sigma_M}{10} \right) \left(\frac{\Gamma}{10} \right)^{-2} \left(\frac{L_{\text{tot}}}{10^{-4} \text{ erg/cm}^3} \right)^{-1} \text{ pc}. \quad (104)$$

Thus, for $\Gamma \sim \sigma_M \sim 10$ obtained recently by Nokhrina et al. (2015) from analysis of about 100 sources using core-shift techniques, the distance is quite reasonable to explain the observable retardation on the scale $R \sim 100 \text{ pc}$.

On the other hand, on the scale $R \sim 10 \text{ kpc}$, corresponding to dimension of the galaxy, where $U_{\text{iso}} \sim 10^{-10} \text{ erg/cm}^3$, the retardation length L_{dr} is too large to prevent the jet material reaching the lobes. To conclude, in our opinion, isotropic photon field can be considered as one of the possible reason of jet deceleration in active galactic nuclei.

Finally, it is very interesting to discuss the photon drag action in connection with Fanaroff & Riley (1974) classification. At first glance, deceleration is to be more effective in FR II objects, i.e., in objects in which the ambient radiation field is more intense. But as was demonstrated above, in objects with higher magnetization σ_M , the drag force acts indirectly diminishing mainly the electromagnetic flux. As far as FRI sources, in which one can expect particle dominated flow in parsec scales, drag is to be much more effective. We are going to consider the statistics of the sources in Paper III.

ACKNOWLEDGMENTS

We would like to acknowledge M. Barkov, E. Derishev, Ya. Istomin and especially N. Zakamska for useful comments. We also thank the anonymous referee for his/her helpful remarks. This work was supported by Russian Science Foundation, grant 16-12-10051.

REFERENCES

- Aharonian F.A., Bogovalov S.V., Khangulyan D., 2012, *Nature*, 482, 507
 Appl S., Camenzind M., 1992, *A&A*, 256, 354
 Barkov M.V., Komisarov S.S., 2016, *MNRAS*, 458, 1939
 Beal J.H., Guillori J., Rose D.V., 2010, *Mem. Soc. Astron. Ital.*, 81, 404
 Begelman M.C., Blandford R.D., Rees M.J., 1984, *Rev. Mod. Phys.*, 56, 255
 Benford G., 1981, *ApJ*, 247, 792
 Beskin V.S., 2009, *MHD Flows in Compact Astrophysical Objects*. Springer, Berlin
 Beskin V.S., 2010, *Physics-Uspekhi*, 53, 1199
 Beskin V.S., Gureich A.V., Istomin Ya.N., 1993, *Physics of the Pulsar Magnetosphere*. Cambridge University Press, Cambridge
 Beskin V.S., Kuznetsova I.V., Rafikov R.R., 1998, *MNRAS*, 299, 341
 Beskin V.S., Nokhrina E.E., 2006, *MNRAS*, 367, 375
 Beskin V.S., Nokhrina E.E., 2016, *MNRAS* (in preparation)
 Beskin V.S., Rafikov R.R., 2000, *MNRAS*, 313, 433
 Beskin V.S., Zakamska N.L., Sol H., 2004, *MNRAS*, 347, 587
 Bing Z., Huirong Ya., 2011, *ApJ*, 726, 90Z
 Blumethal G.R., Gould R.G., 1970, *Rev. Mod. Phys.*, 42, 237
 Bogovalov S.V., Khangulyan D.V., Koldoba A.V., Ustyugova G.V., Aharonian F.A., 2008, *MNRAS*, 387, 63
 Bogovalov S.V., Khangulyan D.V., Koldoba A.V., Ustyugova G.V., Aharonian F.A., 2008, *MNRAS*, 419, 211
 Bogovalov S.V., Tsinganos K., 1999, *MNRAS*, 305, 211
 Bucciantini N., Quataert E., Metzger B.D., Thompson T.A., Arons J., del Zanna L., 2006, *ApJ*, 396, 2038
 Cerutti B., Philippov A.A., Parfrey K., Spitkovsky A., 2015, *MNRAS*, 448, 606
 de la Cita V.M., Bosch-Ramon V., Paredes-Fortuni X., Khangulyan D., Perucho M., 2016, *A&A* (in press) arXiv:1604.02070v1
 Clausen-Brown E., Savolainen T., Pushkarev A.B., Kovalev Y.Y., Zensus J.A., 2013, *A&A*, 558, A144
 Cohen M.H. et al, 2007, *ApJ*, 658, 232
 Derishev E.V., Aharonian F.A., Kocharovskiy V.V., Kocharovskiy V.I., 2003, *Phys. Rev. D*, 68, 043003
 Double G.P., Baring M.G., Jones F.C., Ellison D.C., 2004, *ApJ*, 600, 485
 Drenkhahn G., Spruit H.C., 2002, *A&A*, 391, 1141
 Fanaroff B.L., Riley J.M., 1974, *MNRAS*, 167, 31P
 Ferraro V.C.A., 1937, *MNRAS*, 97, 458
 Gabuzda D., Murrey E., Cronin P., 2005, *MNRAS*, 351, 8
 Golan O., Levinson A., 2015, *ApJ*, 809, 23
 Goldreich P., Julian W.H., 1969, *ApJ*, 157, 869

- Goldreich P., Julian W.H. 1969, ApJ, 160, 971
 Hardee P.E., Norman M.L., 1988, ApJ, 334, 70
 Heyvaerts J., Norman J., 1989, ApJ, 347, 1055
 Hirokani K., Okamoto I., 1998, ApJ, 497, 563
 Homan D.C., Lister M.L., Kovalev Y.Y., Pushkarev A.B., Savolainen T., Kellermann K.I., Richards J.L., Ros E., 2014, ApJ, 798, 16
 Istomin Ya.N., Pariev V.I., 1994, MNRAS, 267, 629
 Joshi M., Marscher A.P., Bottcher M., 2014, ApJ, 785, 132
 Kardashev N.S., Novikov I.D., Lukash V.N. et al. 2014, Phys. Uspekhi, 57, 1199
 Kennel C. F., Fujimura F. S., Okamoto I., 1983, Geophys. Astrophys. Fluid Dyn., 26, 147
 Komissarov S., 1994, MNRAS, 269, 394
 Komissarov S., Barkov M., Vlahakis N., Königl A., 2007, MNRAS, 380, 51
 Levinson A. Globus N. 2016, MNRAS, 458, 2269
 Lery T., Heyvaerts J., Appl S., Norman C.A., 1998, A&A, 337, 603
 Li Z.-Y., Begelman M., Chiueh T., 1992, ApJ, 384, 567
 Lobanov A.P., 1998, A&A, 330, 79
 Lyubarskii Yu E., 1999, MNRAS, 308, 1006
 Lyutikov M., 2003, MNRAS, 339, 623
 McKinney J.C., Tchekhovskoy A., Blanford R.D., 2012, MNRAS, 423, 2083
 McKinney J.C., Uzdensky D.A., 2012, MNRAS, 419, 573
 Michel F.C., 1969, ApJ, 158, 727
 Nalewajko K., Begelman M.C., 2012, MNRAS, 427, 2480
 Nokhrina E.E., Beskin V.S., Kovalev Y.Y. Zheltoukhov A.B., 2015, MNRAS, 447, 2726
 Porth O., Fendt Ch., Meliani Z., Vaidya B., 2011, ApJ, 737, 42
 Reynolds C.S., DiMatteo T., Fabian A.C., Hwang U., Canizares C. 1996, MNRAS, 283, L111
 Romanova M.M., Lovelace R.V.E., 1992, A&A, 262, 26
 Russo M., Thompson Ch., 2013a, ApJ, 767, 142
 Russo M., Thompson Ch., 2013b, ApJ, 773, 99
 Rybicki G.B., Lightman A.P., 1981, Radiative Processes in Astrophysics. John Wiley & Sons, New York
 Sikora M., Sol H., Begelman M.C., Madejski G.M., 1996, MNRAS, 280, 781
 Sironi L., Spitkovsky A., 2009, ApJ, 698, 1523
 Stern B.E., Poutanen J., 2006, MNRAS, 372, 1217
 Svensson R., 1984, MNRAS, 209, 175
 Takamoto, Makoto, 2013, ApJ, 775, 50T
 Tchekhovskoy A., Bromberg O., 2016, MNRAS, 461, L46
 Tchekhovskoy A., McKinney J., Narayan R., 2008, MNRAS, 388, 551
 Tchekhovskoy A., McKinney J., Narayan R., 2009, ApJ, 699, 1789
 Thorne K.S., Price R.H., Macdonald D. 1986, Black Holes: The Membrane Paradigm. Yale University Press, New Haven and London
 Ustyugova G.V., Koldoba A.V., Romanova M.M., Chechetkin V.M., Lovelace R.V.E., 1995, ApJ, 439, L39
 Del Zanna L., Papini E., Landi S., Bugli M., Bucciantini N., 2016, arXiv:1605.06331

APPENDIX A: LINEARIZATION IN THE DRIFT APPROXIMATION

In this Appendix we determine the linear disturbances to the cylindrical drag-free flow in the drift approximation. First, using the definitions (36)–(38) for the total magnetic field \mathbf{B} and clear expressions $\mathbf{V}_{\parallel} = (\mathbf{V}\mathbf{B})\mathbf{B}/B^2$ and $\mathbf{V}_{\perp} = \mathbf{V} - \mathbf{V}_{\parallel}$ for any vector \mathbf{V} , we obtain for the perpendicular components of vectors $\mathbf{e} = \mathbf{E}/B_0$ and \mathbf{F}_{dr}

$$e_{\perp}^r = -x - x_0 \frac{1}{r_{\perp}} \frac{\partial}{\partial r_{\perp}} (r_{\perp}^2 \delta), \quad (\text{A1})$$

$$e_{\perp}^{\varphi} = \frac{x}{(x^2 + 1)} \left(\frac{1}{2} x r_{\perp} \frac{\partial f}{\partial z} - x_0 r_{\perp} \frac{\partial \delta}{\partial z} \right), \quad (\text{A2})$$

$$e_{\perp}^z = -x_0 r_{\perp} \frac{\partial \delta}{\partial z} - \frac{1}{x^2 + 1} \left(\frac{1}{2} x r_{\perp} \frac{\partial f}{\partial z} - x_0 r_{\perp} \frac{\partial \delta}{\partial z} \right), \quad (\text{A3})$$

$$F_{\perp}^{\varphi} = -\frac{F_d \gamma^2}{\sqrt{1 - 2\xi_z + \xi_{\varphi}^2}} \frac{(x + \xi_{\varphi})}{1 + x^2}, \quad (\text{A4})$$

$$F_{\perp}^z = -\frac{F_d \gamma^2 x}{\sqrt{1 - 2\xi_z + \xi_{\varphi}^2}} \frac{(x + \xi_{\varphi})}{1 + x^2}, \quad (\text{A5})$$

$$F_{\perp}^r = 0. \quad (\text{A6})$$

Using now these expressions we can obtain for r -component of the drift velocity

$$\xi_r^{\text{dr}} = -\frac{(x + \xi_{\varphi})}{(x^2 + 1)} F_d \gamma^2 - \frac{x x_0 r_{\perp}}{(x^2 + 1)} \frac{\partial \delta}{\partial z}, \quad (\text{A7})$$

and for r -component of longitudinal velocity

$$(\xi_{\parallel})_r = -\frac{1}{2} \frac{(1 - x \xi_{\varphi})}{(1 + x^2)} r_{\perp} \frac{\partial f}{\partial z}. \quad (\text{A8})$$

Substituting these expressions into (47)–(48) and remembering that $\xi_{\varphi} \approx x P_+$, we result in (67).

Further, combining (43), (47)–(48), and (67), one can find

$$\begin{aligned} r_{\perp} \frac{\partial \zeta}{\partial z} &= 4K r_{\perp} \frac{\Omega_0}{\Omega_F} \frac{\partial \delta}{\partial z} \\ &- F_d \Gamma^2 \left[1 - \frac{(1 - x^2 P_+)^2}{(1 + x^2)} \right] \frac{\Omega_0}{\Omega_F} \frac{r_{\text{jet}}^2}{r_{\perp}} + \\ &+ \frac{4K \Omega_0}{r_{\perp} \Omega_F} \frac{(1 - x^2 P_+)}{(1 + x^2)} \left(-r_{\perp}^2 \frac{\partial \delta}{\partial z} + r_{\perp}^2 \frac{\Omega_F}{2\Omega_0} \frac{\partial f}{\partial z} \right), \end{aligned} \quad (\text{A9})$$

where we put $(\gamma^+)^2 + (\gamma^-)^2 = 2\Gamma^2$. Integrating it, we obtain

$$\zeta = \frac{A}{\sigma} \int F_d \Gamma^2 dz + 4K \frac{x x_0}{(x^2 + 1)} \delta + 2K \frac{(1 - x^2 P_+)}{(1 + x^2)} f, \quad (\text{A10})$$

where A is given by (88). Finally subtracting equation (46) from (45) and neglecting l.h.s., one can obtain the following expression

$$q_+ = x p_+ + \frac{1}{R_L} \frac{\partial}{\partial r_{\perp}} (r_{\perp}^2 \delta) - x_0 \zeta, \quad (\text{A11})$$

where again $R_L = c/\Omega_0$ is the light cylinder radius.

Finally, using definitions (56)–(58) and expressing γ^+ and γ^- through Γ and G , we have

$$\frac{1}{(\Gamma + G/2)^2} = 2 \left(P_+ + \frac{P_-}{2} \right) - \left(Q_+ + \frac{Q_-}{2} \right)^2, \quad (\text{A12})$$

$$\frac{1}{(\Gamma - G/2)^2} = 2 \left(P_+ - \frac{P_-}{2} \right) - \left(Q_+ - \frac{Q_-}{2} \right)^2. \quad (\text{A13})$$

They give for $G \ll \Gamma$

$$G = -\Gamma^3(1 - x^2 P_+)P_-, \quad (\text{A14})$$

and

$$g_- = -(1 - x^2 P_+)\Gamma^3 p_- + x P_- \Gamma^3 q_+. \quad (\text{A15})$$

These relations lead to a system of equations (75)–(83).

As a result, expressing p_+ from (77) and substituting it together with ζ in (76), we obtain

$$q_+ = -\frac{x}{\Gamma^3(1 - x^2 P_+)}g_+ + \frac{1}{(1 - x^2 P_+)}\frac{1}{R_L}\frac{\partial}{\partial r_\perp}(r_\perp^2 \delta) + \frac{x_0}{(1 - x^2 P_+)}\left[\frac{A}{\sigma}\Gamma^2(F_{dz}) - \frac{4Kxx_0}{(1 + x^2)}\delta - \frac{2K(1 - x^2 P_+)}{(1 + x^2)}f\right] \quad (\text{A16})$$

Put it in (83), we obtain

$$4\lambda x x_0 p_- + r_\perp \frac{\partial}{\partial r_\perp} \left[\frac{1}{r_\perp} \frac{\partial}{\partial r_\perp} (r_\perp^2 f) \right] + \frac{16K^2 x_0^2}{(1 + x^2)}f + \frac{32K^2 x_0^3 x}{(1 - x^2 P_+)(1 + x^2)}\delta - \frac{8Kx_0^2}{(1 - x^2 P_+)}\frac{1}{r_\perp} \frac{\partial}{\partial r_\perp} (r_\perp^2 \delta) + r_\perp^2 \frac{\partial^2 f}{\partial z^2} = \frac{8Kx_0^2}{(1 - x^2 P_+)}\frac{A}{\sigma}\mathcal{G} - \frac{8Kxx_0(1 - x^2 P_+)}{1 + x^2}\frac{\mathcal{G}}{\Gamma^3}, \quad (\text{A17})$$

where $\mathcal{G} = \Gamma^2(F_{dz})$. Besides, substituting (81) into (82) and expressing p_+ , we get the second equation

$$2\lambda p_- + \frac{16K^2 x_0^2 P_+(x^2 + 1 - x^2 P_+)}{(1 + x^2)(1 - x^2 P_+)}\delta + r_\perp^2 \frac{\partial^2 \delta}{\partial z^2} + \frac{1}{r_\perp} \frac{\partial}{\partial r_\perp} \left[r_\perp \frac{\partial}{\partial r_\perp} (r_\perp^2 \delta) \right] - \frac{4}{r_\perp} \frac{\partial}{\partial r_\perp} \left[r_\perp^2 K \frac{xx_0}{(1 + x^2)}\delta \right] - \frac{2}{r_\perp} \frac{\partial}{\partial r_\perp} \left[r_\perp^2 K \frac{(1 - x^2 P_+)}{1 + x^2}f \right] - \frac{4Kxx_0 P_+}{(1 - x^2 P_+)}\frac{1}{r_\perp} \frac{\partial}{\partial r_\perp} (r_\perp^2 \delta) = -\frac{1}{r_\perp} \frac{\partial}{\partial r_\perp} (r_\perp^2 \frac{A}{\sigma}\mathcal{G}) + \frac{4Kxx_0 P_+}{(1 - x^2 P_+)}\frac{A}{\sigma}\mathcal{G} + \frac{4K(1 - x^2 P_+)}{\Gamma^3(1 + x^2)}\mathcal{G}. \quad (\text{A18})$$

Neglecting now longitudinal derivatives $\partial^2/\partial z^2$ one can rewrite the system of equations (A17)–(A18) as two second-order ordinary differential equations for $D = x_0^2 \delta$ and $F = x_0 f$

$$\frac{d^2 D}{dx_0^2} = -\frac{1}{x_0} \frac{dD}{dx_0} + \frac{1}{x_0} \frac{dY}{dx_0} - 2\lambda p_- + 4Kp_+, \quad (\text{A19})$$

$$\frac{d^2 F}{dx_0^2} = -\left[\frac{1}{x_0} + 2x \frac{d}{dx_0} \left(\frac{1}{x} \right) \right] \frac{dF}{dx_0} - 4\lambda x^2 p_- + 8Kxq_+ - \left[x \frac{d^2}{dx_0^2} \left(\frac{1}{x} \right) + \frac{x}{x_0} \frac{d}{dx_0} \left(\frac{1}{x} \right) - \frac{1}{x_0^2} \right] F. \quad (\text{A20})$$

Here $Y = x_0^2 \zeta$,

$$Y = \frac{4Kxx_0}{(1 + x^2)}D + \frac{2Kx_0(1 - x^2 P_+)}{x(1 + x^2)}F - \frac{Ax_0^2}{\sigma_M}\mathcal{G}, \quad (\text{A21})$$

$\mathcal{G} = \Gamma^2(F_{dz})$, and

$$\lambda p_- = \frac{8\lambda^2 \sigma_M}{\Gamma^3 x_{\text{jet}}^2 (1 + x^2)} \left(D - \frac{1}{2}F \right) + \frac{2KP_+ x}{(1 + x^2)}\frac{\mathcal{G}}{\Gamma^3} + \frac{2KP_+}{(1 - x^2 P_+)^2} \frac{\partial}{\partial x_0} D - \frac{2KP_+}{x_0(1 - x^2 P_+)^2} Y, \\ p_+ = \frac{(1 - x^2 P_+)}{(1 + x^2)}\frac{\mathcal{G}}{\Gamma^3} + \frac{xP_+}{(1 - x^2 P_+)}\frac{\partial}{\partial x_0} D - \frac{xP_+ Y}{x_0(1 - x^2 P_+)}, \\ q_+ = \frac{(1 - x^2 P_+)x}{\Gamma^3(1 + x^2)}\mathcal{G} + \frac{1}{(1 - x^2 P_+)}\frac{dD}{dx_0} - \frac{Y}{x_0(1 - x^2 P_+)} \quad (\text{A22})$$

Outside the light cylinder $x_0 \gg 1$ it gives

$$\frac{d^2}{dx^2} \left(D - \frac{F}{2} \right) - \frac{16\lambda^2 \sigma_M}{\Gamma^3 x_{\text{jet}}^2} \left(D - \frac{F}{2} \right) + \dots = 0. \quad (\text{A23})$$

Hence, the physical branch of equations (A19)–(A20) corresponds to fastly diminishing solution $(D - F/2) \rightarrow 0$ with the spacial scale $\Delta x \ll 1$

$$(\Delta x)^2 = \frac{\Gamma^3 x_{\text{jet}}^2}{16\lambda^2 \sigma_M}. \quad (\text{A24})$$

Finally, for $D = F/2$, i.e., in the one-fluid MHD approximation ($E_\parallel = 0$) Eqns. (A17)–(A18) result in (86)–(87). Expressing now p_- from (A17) and put it into (A18), we finally obtain Eqn. (101).

APPENDIX B: TOY MODEL

Boundary condition $D(0) = 0$ to equation (101) is actually one of the key nontrivial property of the solution discussed above. The point is that any finite central engine with dipole-like magnetic field produces quadrupole electric field so that the potential difference between its magnetic pole and infinity does not vanish. On the contrary, our solution corresponds to zero (more exactly, very small) electric field E_z along the rotational axis.

To demonstrate the very possibility for the longitudinal electric field E_z to be small, let us write down by hand the electric potential in the region $z > 0$ (and vanishing at infinity) in the form

$$\Phi_e = \frac{\Omega_0 B_0}{c} r_{\text{jet}}^2 \left(C + \frac{1}{2} \frac{r_\perp^2}{r_{\text{jet}}^2} - \frac{1}{4} \frac{r_\perp^4}{r_{\text{jet}}^4} \right) \exp \left(-\frac{z^2}{L_{\text{dr}}^2} \right), \quad (\text{B1})$$

where we use the expression (102) for angular velocity Ω_F . For $L_{\text{dr}} \rightarrow \infty$ it corresponds to electric field $E_r^{(0)}$ (23) for arbitrary constant C . In particular, it gives the same zero-order charge density ρ_e (32). As was already stressed, $C < 0$ ($|C| \sim 1$) for $L_{\text{dr}} \rightarrow 0$, i.e. for spatially limited quadrupole charge distribution.

On the other hand, for finite L_{dr} the disturbance of charge density in the vicinity of the rotational axis for $z \sim r_{\text{jet}}$ depends drastically on constant C . Indeed, the additional charge density can be divided into two terms, namely, the negative part

$$\delta \rho_e^{(1)} = -|C| \frac{\Omega_0 B_0}{2\pi c} \frac{r_{\text{jet}}^2}{L_{\text{dr}}^2} \quad (\text{B2})$$

existing for $C \neq 0$ (and producing electric field $E_z < 0$ along the rotation axis opposite the particle flow), and the positive one

$$\delta \rho_e^{(2)} = \frac{\Omega_0 B_0}{2\pi c} \frac{z^2}{L_{\text{dr}}^2} \quad (\text{B3})$$

having the same order of magnitude on the scale $z \sim r_{\text{jet}}$. This implies that the small redistribution of the charge density in the base of the flow indeed can screen the longitudinal electric field along the jet.